AJNR

MR Findings in Spinal Hemangioblastoma: Correlation with Symptoms and with Angiographic and Surgical Findings

Bao-Cheng Chu, Satoshi Terae, Kazutoshi Hida, Matakazu Furukawa, Satoru Abe and Kazuo Miyasaka

AJNR Am J Neuroradiol 2001, 22 (1) 206-217
http://www.ajnr.org/content/22/1/206

AJNR Am J Neuroradiol 22:206–217, January 2001

MR Findings in Spinal Hemangioblastoma: Correlation with Symptoms and with Angiographic and Surgical Findings

Bao-Cheng Chu, Satoshi Terae, Kazutoshi Hida, Matakazu Furukawa, Satoru Abe, and Kazuo Miyasaka

BACKGROUND AND PURPOSE: **To our knowledge, a detailed analysis of MR findings in spinal hemangioblastoma has not been conducted to date. Our purpose was to elucidate the MR features of this disease with special attention to tumor size, correlation with MR findings and clinical symptoms, and any differences between patients with and without von Hippel-Lindau disease (VHLD).**

METHODS: **MR images in five patients with VHLD and seven patients without VHLD were reviewed retrospectively for spinal hemangioblastoma by two neuroradiologists. The MR findings were correlated with clinical symptoms and with angiographic and surgical findings.**

RESULTS: **The MR features depended on the size of the spinal hemangioblastoma. Small (10 mm or less) hemangioblastomas were mostly isointense on T1-weighted images, hyperintense on T2-weighted images, and showed homogeneous enhancement. Larger hemangioblastomas tended to be hypointense or mixed hypo- and isointense on T1-weighted images, heterogeneous on T2-weighted images, and tended to show heterogeneous enhancement. Small hemangioblastomas were located at the surface of the spinal cord, most frequently along its posterior aspect. These were subpial in location at surgery and showed well-demarcated, intense enhancement. Symptomatic small hemangioblastomas had relatively large associated syringes, whereas asymptomatic ones did not. A hemangioblastoma larger than 24 mm was invariably accompanied by vascular flow voids. There was no difference in the MR findings between the two patient groups except for the multiplicity and higher percentage of small tumors in patients with VHLD.**

CONCLUSION: **Knowledge of these MR features helps to differentiate spinal hemangioblastoma from other diseases that show enhancing nodules.**

Imaging findings in spinal hemangioblastoma have been reported for studies performed with myelography, CT, and angiography (1–4). Although MR imaging has become the radiologic study of choice for spinal tumors, published reports on the MR findings in spinal hemangioblastoma have been based on relatively few cases (3–13). In this study, we evaluated the MR findings in spinal hemangioblastoma in 12 patients to determine the characteristic MR features and to compare these with clinical symptoms and with angiographic and surgical findings. We also compared the MR findings in spinal hemangioblastoma in patients with von Hippel-Lindau disease (VHLD) against those in patients with sporadic hemangioblastomas.

Received February 14, 2000; accepted after revision June 26.

From the Departments of Radiology (B-C.C., S.T., M.F., K.M.) and Neurosurgery (K.H.), Hokkaido University School of Medicine; and the Department of Radiology, Sapporo Azabu Neurosurgical Hospital (S.A.), Sapporo, Japan.

Address reprint requests to Satoshi Terae, MD, Department of Radiology, Hokkaido University, School of Medicine, Sapporo, 060-8638, Japan.

Methods

Twelve consecutive patients with spinal hemangioblastoma were treated between November 1989 and March 2000. In five patients (two men and three women, aged 16–49 years), the hemangioblastomas were associated with VHLD. Of these five patients, three were confirmed to have spinal hemangioblastoma at surgery. In the other two patients, diagnosis of spinal hemangioblastoma was based on the exclusion of other diseases, such as metastasis and sarcoidosis, by laboratory tests, general imaging studies, and follow-up MR examinations. In seven patients (five men and two women, aged 30–59 years) hemangioblastoma was not associated with VHLD, and in all seven of these, hemangioblastoma was proved at surgery.

The primary symptoms in nine of the 12 patients included pain, proprioceptive sensation disturbance of position and vibration, motor weakness, and bowel and urinary dysfunction (Table). Two patients with VHLD had no subjective symptoms; however, neurologic examination revealed sensory disturbance in one of them. In one patient without VHLD, a hemangio-

Summary of clinical manifestations

Case No.	Sex/Age (y)	Duration	Neurologic Symptoms	Other Disease Processes
1	M/16	5	Bowel and urinary incontinence, hypalgesia and hypesthesia (below C2), tetraparesis	VHLD, CH
2	F/42	· · ·	No subjective symptoms (hypalgesia and decreased position sense in bilateral L/E)	VHLD, RCC
3	F/24	4 mo	Pain in L foot	VHLD, RCC
4	F/44	· · ·	Asymptomatic	VHLD, RCC, CH, RH
5	M/49	30 y	Pain, weakness, and decreased vibration sense in bilateral L/E	VHLD, RCC
6	M/30	5 y	Paraparesis, hypalgesia, and hypesthesia (below T8); decreased vibration and position sense in bilateral L/E; bowel and urinary incontinence	· · ·
7	F/49	6 y	Pain in L shoulder, dysesthesia in face, weakness of L U/E; decreased vibration and position sensation in L U/E	· · ·
8	F/59	10 y	Tetraparesis and hypalgesia in bilateral U/E and L/E; decreased vibration sense in bilateral L/E	· · ·
9	M/52	1 y	Brown-Séquard syndrome	· · ·
10	M/41	2 y	Weakness and numbness in R hand; bowel and urinary incontinence	· · ·
11	M/44	7 mo	Decreased deep sense in L L/E; bowel and urinary incontinence	· · ·
12	M/44	· · ·	Asymptomatic (pain in R leg due to herniated disk at L5–S1)	· · ·

Note.—L/E indicates lower extremities; U/E, upper extremities; VHLD, von Hippel Lindau disease; CH, cerebellar hemangioblastoma; RCC, renal carcinoma; RH, retinal hemangioblastoma.

blastoma was found incidentally at MR examination performed for lumbar disk herniation. This patient had no symptoms related to the tumor.

MR examinations were performed on 1.5-T units using a spinal coil. Spin-echo (SE) or fast spin-echo (FSE) or turbo spin-echo (TSE) T1-weighted imaging was performed in the sagittal plane in 11 patients and in the axial plane in eight. T2-weighted imaging was performed in the sagittal plane in 10 patients and in the axial plane in seven. Contrast material was injected intravenously at a dose of 0.1 mmol/kg body weight to obtain contrast-enhanced T1-weighted images in both sagittal and axial planes in 11 patients, and in the sagittal plane only in the remaining patient. TR/TE was 500–800/12–20 for the SE T1-weighted images and 2200/90 for the SE T2-weighted images. TR/TE_{eff} was 600–700/10–12 for the TSE or FSE T1-weighted images, 4100–6220/80–112 for the TSE or FSE T2-weighted images. Slice thickness was 3 to 5 mm with an interslice gap of 0.3 to 0.5 mm for the sagittal plane, and 5 mm with variable interslice gaps for the axial plane.

Images were reviewed by two neuroradiologists who were blinded to the angiographic and surgical findings. The MR images were then evaluated for the following criteria: location, shape, size, signal intensity, enhancement pattern, marginal definition of the tumor, vascular flow voids, superficial enhancement of the spinal cord, syrinx or cyst, and edema. Tumor location was classified into four groups: intramedullary, intra- and extramedullary, intradural extramedullary, and extradural. In cases of intramedullary tumors, the location was further divided into superficial or deep groups. In cases of superficially located tumors, the location was further divided into posterior, lateral, or anterior aspects. The location was defined as intra- and extramedullary if an extramedullary component was observed in continuity with an intramedullary component. The maximal diameter of a tumor was measured by using calipers. Signal intensity was characterized as hypo-, hyper-, or isointense relative to signal intensity of normal-appearing spinal cord. The enhancement of a tumor was recorded as homogeneous or heterogeneous with respect to the texture, and as intense, moderate, or mild with respect to the intensity. Intense enhancement was defined as that which was equal to or higher than the signal intensity of subcutaneous fat or of epidural venous plexus on contrast-enhanced T1-weighted images. Tumors were classified as well demarcated or poorly demarcated depending on the relationship between enhancing tumor and adjacent tissue. Generally, it is difficult to distinguish cyst from syrinx even on histopathologic specimens; therefore, in this study, we defined a syrinx as a cystic cavity larger than one vertebral segment in length and containing fluid. A peritumoral cyst was defined as a cystic cavity adjacent to the tumor and confined within one vertebral segment. It was mandatory that neither cystic cavity showed enhancement of the wall of the cavity. Edema was represented as a pencil-shaped intramedullary lesion with blurry margins that was hypointense on T1-weighted images, hyperintense on T2-weighted images, and showed no contrast enhancement.

MR findings were correlated with clinical symptoms and with angiographic findings, which were available in six patients. The feeders, tumor stain, and draining veins were identified by reviewing the angiograms. The MR findings were also compared with the surgical findings, which were available in 10 tumors in nine patients, with respect to tumor location, feeding vessels and draining veins, and presence of syrinx and edema.

Results

A total of 32 tumors were found in the 12 patients. Among the five patients with VHLD, four had multiple tumors and one had a solitary tumor (total, 25 tumors). The seven patients without VHLD all had a solitary tumor.

Tumor Location

Ten (31%) tumors were located in the cervical region, two in cervicothoracic region, 16 (50%) in the thoracic region, one in the thoracolumbar region, two in the lumbar region, and one in the sacral region.

Of the 32 tumors, 24 were intramedullary in location. Two were intra- and extramedullary, and these were 60 and 17 mm in size, respectively (Fig 1). One tumor, which was 15 mm in size, was intradural and extramedullary. One tumor, 25 mm in size, was located at the left extradural S1 nerve (Fig 2), and three small tumors were located along the dorsal nerve root to the cord surface (Fig 3). The location of one tumor could not be determined because transverse slices were not obtained. Of the 24 intramedullary tumors, 21 (88%) were located superficially, most frequently at the posterior aspect of the spinal cord (n = 16) (Fig 4) and occasionally at the anterior aspect (n = 4) (Fig 5) or the posterolateral aspect (n = 1). As for the small intramedullary tumors (10 mm or less in size), 18 (95%) of 19 were superficial in location (Figs 4–7). There was no significant difference between patients with and without VHLD as to whether the tumor was located intramedullary or completely extramedullary (Fisher's exact test; $P = .69$).

Tumor Shape and Size

Of the 25 tumors in the patients with VHLD, 23 were small (10 mm or less), and nodular or ovoid in shape. They were located intramedullary or along the dorsal nerve root (Figs 3–6 and 8). One intramedullary tumor was sausagelike and measured 60 mm along its major axis (Fig 6). The one remaining extradural S1 nerve tumor was round and 25 mm in size (Fig 2).

Of the seven tumors in the patients without VHLD, two were nodular and less than 10 mm in size and located superficially at the spinal cord (Fig 7). Three were ovoid and 15 to 17 mm in size. One was 40 mm, and the remaining one was 60 mm along the major axis (Fig 1). The percentage of occurrence of small tumors (10 mm or less) was significantly higher in the patients with VHLD than in those without VHLD (Fisher's exact test; $P = .002$).

Signal Intensity of the Tumor

T1- and T2-weighted images were available for 22 and 21 tumors, respectively. Signal intensity was described for the tumor parenchyma, excluding vascular flow voids. On T1-weighted images, 16 tumors were isointense with surrounding tissue, five were of low signal intensity, and one showed mixed low intensity and isointensity. On T2-weighted images, 14 tumors showed high signal intensity, three were isointense, and four were of mixed high intensity and isointensity or high and low intensity. There was no difference in signal intensity pattern between patients with and without VHLD. However, signal intensity corresponded to the size of the tumor: among small tumors (10 mm or less), all but one (14 of 15) were isointense on T1-weighted images and all but two (13 of 15) were of high signal intensity on T2-weighted images (Fig 7); medium-sized tumors (11–20 mm) tended to be hypointense on T1-weighted images (three of four), and large tumors (>20 mm) were heterogeneous (hyper- and isointense) on T2-weighted images (three of three) (Figs 1 and 2).

Enhancement Pattern and Marginal Definition of the Tumors

All tumors showed intense enhancement and were well demarcated from adjacent tissues on contrast-enhanced MR images. Twenty-three tumors showed homogeneous enhancement and nine showed heterogeneous enhancement. The heterogeneous enhancement was caused by vascular flow voids in seven of the nine tumors. The enhancement pattern also corresponded to tumor size. Of the 23 small tumors, 22 showed homogeneous enhancement. Of the nine medium-to-large tumors, eight showed heterogeneous enhancement (Figs 1, 2, 6, and 8).

Vascular Flow Voids

Vascular flow voids were found in seven tumors, ranging in size from 15 to 60 mm (four were intramedullary, the remaining three were either intramedullary with an extramedullary component, intradural extramedullary, or extradural) (Figs 1, 2, and 6). Vascular flow voids were not detected in tumors that were smaller than 15 mm. There were five large tumors, ranging in size from 25 to 60 mm. These large tumors invariably had vascular flow voids in or around the tumor. As for the medium-sized tumors, two (50%) of four were accompanied by vascular flow voids.

Superficial enhancement of the spinal cord was found in four patients, in three of whom the enhancement was associated with vascular flow voids (Figs 1, 6, and 8).

Syrinx or Cyst and Edema

No peritumoral cysts were found in this study. A syrinx was found in seven (64%) of the 11 patients who had a tumor in an intramedullary location or in an intra- and extramedullary location.

Of the five patients with VHLD, three had a syrinx. The syrinx extended over almost the whole spinal cord in two patients, and over two vertebral segments in one (Figs 3 and 6). It was difficult to determine which tumor was responsible for the syrinx formation, because these patients had multiple intramedullary tumors. The size of the largest tumor was 60 mm in one patient (Fig 6) and 15 mm in another. In the remaining patient with a small syrinx, the tumor adjacent to the syrinx was 2 mm in size and was located at the surface of the spinal cord. Edema was observed in four patients. In two of these, the edema was adjacent to the syrinx (cases 2 and 5) (Fig 3); in the other two, the edema

FIG 1. Case 6: 30-year-old man without VHLD.

A and *B,* Sagittal T1-weighted SE images (400/23/2) before (*A*) and after (*B*) intravenous administration of contrast material show a large, sausagelike, well-demarcated, intensely but heterogeneously enhancing tumor at T12–L1. Note superficial enhancement of the spinal cord (*arrows, B*), confirmed to be dilated perimedullary veins at surgery. Cephalic portion of the tumor resides within the spinal cord, and the caudal portion is extramedullary. A large intramedullary tumor with exophytic growth was confirmed at surgery.

C, Sagittal T2-weighted FSE image (4000/96/3) shows mixed hyper- and isointense tumor. Cephalic to this tumor is syringomyelia up to C2 level (only partially shown). Note prominent vascular flow voids (*arrows*).

D and *E,* Arterial (*D*) and venous (*E*) phases of digital subtraction angiograms, anteroposterior view, with right T10 intercostal artery catheterized, show intense tumor stain at T12–L1, dilated posterior spinal artery as a feeder (*straight arrows, D*), and dilated draining vein (*curved arrows, E*).

was not associated with the syrinx, but rather with a small tumor (6 and 10 mm in size, respectively) and extended over three to four vertebral segments (Figs 4 and 5).

Of the seven patients without VHLD, five had syrinx associated with tumor. These tumors were 4, 8, 15, 40, and 60 mm in size, respectively. The syrinx extended over four vertebral segments in the patient who had a 4-mm tumor at the posterior surface of the spinal cord. In the other four patients, the syrinx extended over at least 11 vertebral levels. Edema was observed in three patients. In two patients, edema was adjacent to the syrinx; in the other patient, edema was not associated with syrinx, but rather with a medium-sized tumor (17 mm) and extended over 17 vertebral levels.

Correlation between Clinical Symptoms and MR Findings

Clinical symptoms were correlated with tumor size and location, syrinx, and edema. All patients with VHLD had at least one asymptomatic tumor. In cases 1, 2, and 5, multiple small tumors were

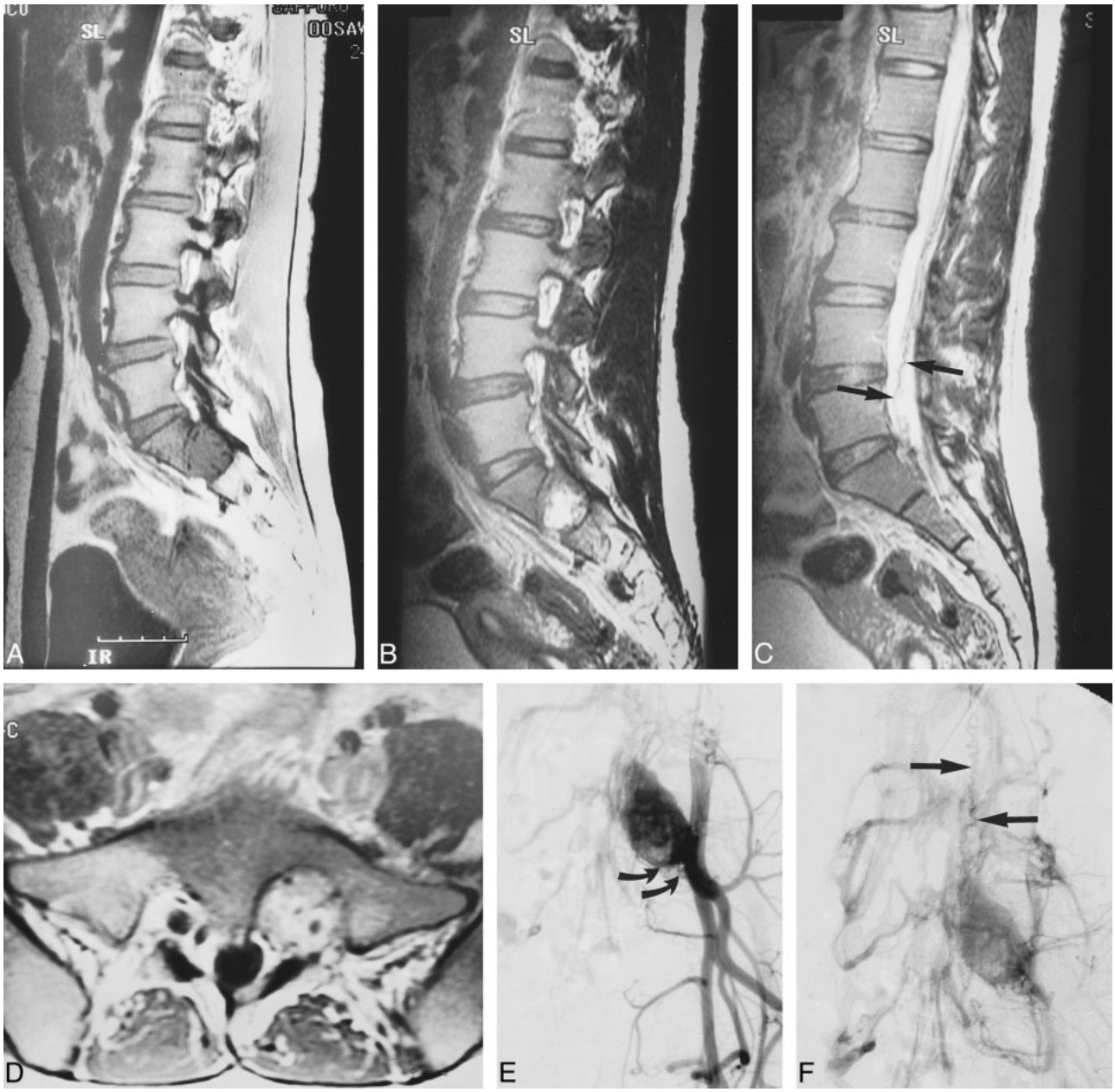

FIG 2. Case 3: 24-year-old woman with VHLD.

A, Sagittal T1-weighted FSE image (700/10/6) shows a large, round, hypointense tumor in the left vertebral foramen between S1 and S2. Note vascular flow voids within the tumor.

B, Sagittal T2-weighted FSE image (4100/121/5) shows mixed iso- and hyperintense tumor.

C, Sagittal T2-weighted FSE image (4100/121/5), medial to slice in *B,* shows serpentine vascular flow voids (*arrows*).

D, Contrast-enhanced axial T1-weighted FSE image (740/8.6/4) shows intensely but heterogeneously enhancing tumor that was confirmed to arise from left S1 nerve root at surgery.

E and *F,* Arterial (*E*) and venous (*F*) phases of digital subtraction angiograms, right anterior oblique 30° view, with left internal iliac artery catheterized, show intense tumor stain, dilated lateral sacral arteries that supply the tumor (*curved arrows, E*), and early venous filling (*straight arrows, F*), indicating the arteriovenous shunt in the tumor. This vein corresponds with the flow voids seen in *C.*

observed. In these patients, clinical symptoms were attributable mainly to the syrinx. In two of them, edema was associated with the syrinx and it was possible, although not definite, that the edema was also a cause of the presenting symptoms. In case 1, the large size of the tumor (60 mm) was also partly responsible for the symptoms. On the other hand, in cases 3 and 4, a small intramedullary tumor (10 and 6 mm, respectively) with peritumoral edema at the thoracic spinal cord did not produce symptoms (in case 3, it was the S1 nerve tumor that caused symptoms).

Among the patients without VHLD, one was asymptomatic. This patient had an intradural extramedullary medium-sized tumor (15 mm) but had no syrinx or edema. The tumor was found incidentally on an MR examination performed for lumbar disk herniation. In two patients, clinical symptoms

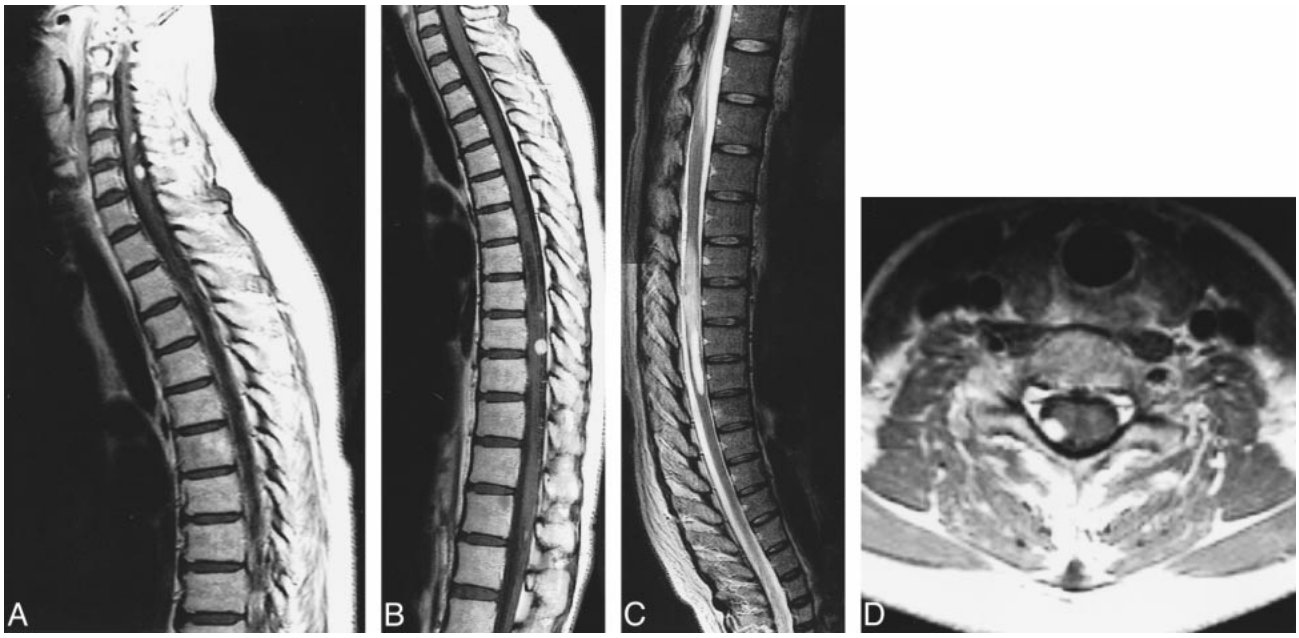

FIG 3. Case 2: 42-year-old woman with VHLD without subjective symptoms.

A and *B,* Contrast-enhanced sagittal T1-weighted FSE images (600/12/6) show nodular, intensely and homogeneously enhancing tumors at the posterior aspects of the spinal cord at levels C5, C6, T8–T9, and T9–T10.

C, Sagittal T2-weighted TSE image (4500/112/3) shows a syrinx at T7–T8 and adjacent edema at T9–T10. This image is a composite of the upper and lower halves of the MR images of the spine.

D, Contrast-enhanced axial T1-weighted TSE image (1000/12/2) shows the tumor surrounding a posterior nerve root at C6, as is also the case with other tumors at C5 and C7–T1 (not shown).

were attributable primarily to the syrinx, with intramedullary tumors of 4 and 15 mm, respectively. In one patient with Brown-Séquard syndrome, the symptoms were attributable primarily to the tumor (17 mm in size) and not to the associated edema. In the remaining three patients, with tumors of 8, 40, and 60 mm, respectively, symptoms were attributable both to the tumor itself and to the syrinx.

For both groups of patients, in cases of small tumors (10 mm or less), clinical symptoms were caused by the syrinx. A small tumor without associated syrinx did not cause spinal cord symptoms. Among the patients who had medium-to-large tumors, clinical symptoms were attributable to the tumor itself and/or to the syrinx. Peritumoral edema without syrinx did not contribute to the patients' symptoms.

Correlation between MR and Angiographic Findings

Contrast enhancement of the tumors on MR images was compatible with tumor stain on angiograms in one patient with VHLD and in five patients without VHLD. In the patient with VHLD, vascular flow voids on MR images corresponded to the feeding artery and draining vein on angiograms in one tumor arising from the S1 nerve root (Fig 2). Among the five patients without VHLD, two had vascular flow voids on MR images, corresponding to the feeding arteries and/or draining veins on angiograms (cases 6 and 11; tumor size: 60 and 40 mm, respectively) (Fig 1). In three patients (cases 7, 9, and 10; tumor size: 8, 17, and 15 mm, respectively), no vascular flow voids were noted on MR images, but abnormal vessels were shown on angiograms. The feeding arteries originated from the anterior spinal artery in three tumors and from the posterior spinal artery in four. The draining veins emptied into the anterior spinal vein in two tumors, into the posterior spinal vein in two, and into the radiculomedullary vein in one.

Correlation between MR and Surgical Findings

In the patients with VHLD, one tumor with a superficial location on MR images was confirmed to be subpial in location at surgery. In two tumors seen as deeply located within the spinal cord on MR images, one was confirmed to be deeply located within the cord at surgery (Fig 6) and the other was found to be subpial in location at surgery. In the latter patient, the spinal cord was pushed ventrally by the tumor (15 mm in size), becoming very thin, and the enhancing tumor was located centrally in the dural sac on MR images (Fig 8). One tumor, located within the left S1 nerve on MR images (Fig 2), was confirmed to arise from the S1 nerve at surgery, and was totally excised along with the nerve. In the patients without VHLD, four tumors in superficial locations on MR images were confirmed to be subpial at surgery. Two tumors, both intra- and extramedullary in location, and one tumor, intradural-extramedullary in location on MR images, were proved to have been

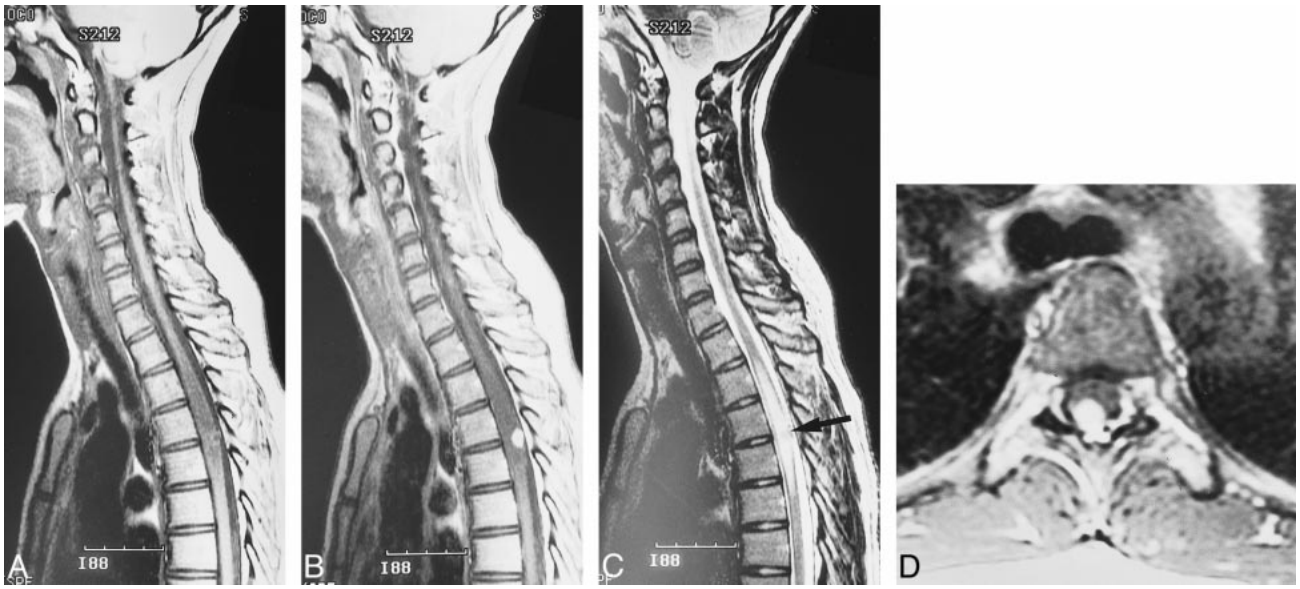

FIG 4. Case 3: 24-year-old woman with VHLD.

A, Sagittal T1-weighted FSE image (700/10/6) shows cord enlargement and decreased signal intensity at T3–T6.

B, Contrast-enhanced sagittal T1-weighted FSE image (700/10/6) shows a small, ovoid, well-demarcated, intensely and homogeneously enhancing tumor at T4–T5.

C, Sagittal T2-weighted FSE image (4220/120/5) shows isointense tumor (*arrow*) and hyperintense pencil-shaped lesion from T3 to T6.

D, Contrast-enhanced axial T1-weighted FSE image (540/9/3) shows the tumor is superficially located at the posterior aspect of the spinal cord.

FIG 5. Case 4: 44-year-old woman with VHLD who had no spinal cord symptoms.

A, Contrast-enhanced sagittal T1-weighted SE image (800/14/2) shows a small, ovoid, well-demarcated, intensely enhancing intramedullary tumor at the anterior aspect of the spinal cord at T10.

B, Sagittal T2-weighted TSE image (4500/112/3) shows edema (*arrow*).

C, Contrast-enhanced axial T1-weighted SE image (660/15/1) shows the tumor is superficially located at the anterior aspect of the spinal cord.

correctly located at surgery (cases 6, 9, and 12) (Fig 1). The extramedullary tumor arose from a posterior nerve root. The superficial enhancement of the spinal cord corresponded to perimedullary draining veins at surgery. The peritumoral cystic cavity was identified by confirming the efflux of fluid after incision of the wall of the cavity.

Intraoperative sonography was used in some of the patients, but the sonographic findings were not included in this study.

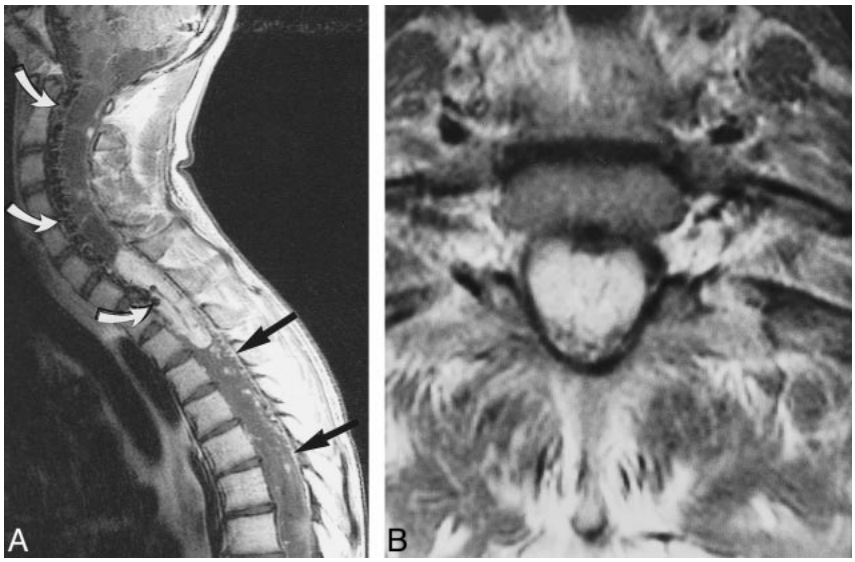

FIG 6. Case 1: 16-year-old boy with VHLD.

A, Contrast-enhanced sagittal T1-weighted TSE image (700/12/2) shows a large, well-demarcated, intensely and heterogeneously enhancing intramedullary tumor at C7–T2. Note vascular flow voids in and around the tumor (*curved arrows*) and superficial enhancement of the spinal cord (*straight arrows*), proved to be dilated perimedullary veins at surgery. Syrinx extends from medulla oblongata to T12. Also note multiple small intensely and homogeneously enhancing tumors, most of which are located superficially at the posterior aspect of the spinal cord.

B, Contrast-enhanced axial T1-weighted SE image (660/15/1) at C7–T1 shows enlargement of the spinal canal and the enhancing tumor. The tumor occupies entire dural sac and the spinal cord is barely discernible. The tumor was interpreted as deeply located within the spinal cord on MR image, and was confirmed at surgery.

MR findings of syrinx and edema were compatible with the surgical findings in all but one tumor (case 6). On MR images, this tumor had edema at C2–C3, which was beyond the surgical field. Pathologically, all hemangioblastomas were densely vascular tumors consisting of thin-walled, closely packed blood vessels interspersed with large stromal cells.

Discussion

Hemangioblastomas of the spinal cord are rare benign tumors representing 1.6% to 6.4% of spinal tumors (1, 7, 14). According to a review of 85 histologically documented case reports by Browne et al (1), about two thirds of spinal hemangioblastomas are sporadic and the remainder are associated with VHLD. The lesions are single in 79% of cases. In patients with VHLD, hemangioblastomas are often multiple. Sixty percent of spinal hemangioblastomas are intramedullary, 11% are intra- and extramedullary, 21% are intradural extramedullary, and 8% are extradural (1). The thoracic spinal cord is most frequently involved (51%), followed by the cervical spinal cord (38%). Forty-three percent of all spinal hemangioblastomas have associated syrinx, and, when only cases of intramedullary spinal hemangioblastoma are considered, 67% have associated syrinx. No MR findings are included in this review.

To our knowledge, no detailed analysis of MR findings in spinal hemangioblastoma has been conducted to date. Previously published MR imaging findings in spinal hemangioblastoma have been based primarily on case reports (3–13). Among these articles, those published before 1989 did not include contrast-enhanced MR studies (4–6, 12). Although Xu et al (14) reported 13 cases of intramedullary hemangioblastoma of the spinal cord, the focus was more on surgical treatment. In a pictorial essay by Baker et al (13), the MR findings were based on a literature review and on some of their own cases; however, their material was not explicitly described. In the present study, we analyzed the MR findings in spinal hemangioblastoma with special attention to the relationship between tumor size and other MR findings, including tumor location, signal intensity, vascular flow voids, associated syrinx, and edema. We compared the MR findings in hemangioblastoma in patients with VHLD with those in sporadic hemangioblastoma to ascertain any differences. We also correlated the MR findings with clinical symptoms and with angiographic and surgical findings.

We found several characteristic MR findings in spinal hemangioblastoma, among which was the finding of well-demarcated, intense enhancement. This property was evident in all tumors in this study (Figs 1–8) and reflects the associated abnormal, densely vascular tumor parenchyma, which consisted of thin-walled, closely packed blood vessels interspersed with large stromal cells.

The second characteristic MR finding was the superficial location of the intramedullary tumors (21/24) (Figs 4–7), most often at the posterior aspect of the spinal cord (16/21) (Figs 3, 4, and 6), reflecting the surgically proved subpial location of the intramedullary tumor. The third characteristic finding was the relatively large size of the syrinx as compared with the size of the intramedullary tumor (Figs 3 and 7). The frequency of syrinx formation was high (64%) in cases of intramedullary tumors. Although syrinx is not specific to spinal hemangioblastomas, as it may be associated with other spinal tumors, such as ependymoma and astrocytoma (13), a small superficially located tumor with a large syrinx is considered characteristic (Figs 3 and 7). Once the tumor was totally removed, the syrinx disappeared or shrunk without the need for additional drainage or for a shunt procedure.

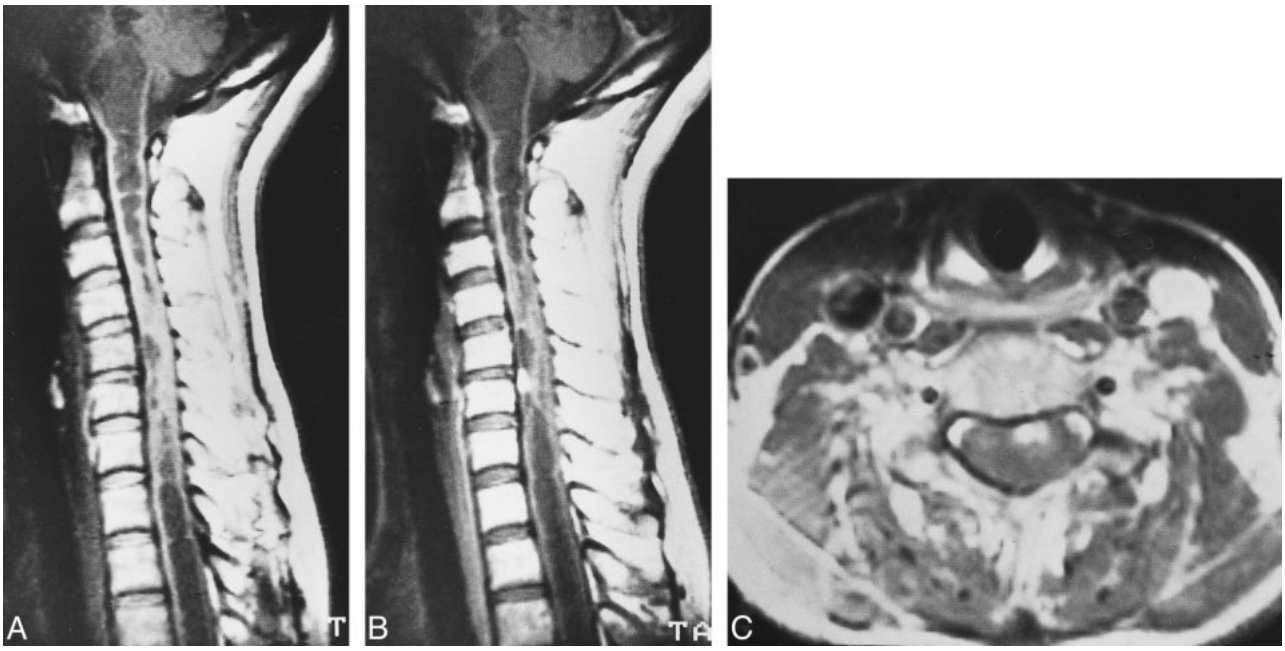

FIG 7. Case 7: 49-year-old woman without VHLD.

A and *B,* Noncontrast (*A*) and contrast-enhanced (*B*) sagittal T1-weighted SE images (600/15/2) show a small, homogeneously and intensely enhancing nodular tumor at C5–C6. The tumor is isointense on noncontrast T1-weighted image. Note extensive syrinx from medulla oblongata to T3 level.

C, Contrast-enhanced axial T1-weighted SE image (600/15/2) shows the tumor is well demarcated, superficially located at the anterior aspect of the spinal cord.

FIG 8. Case 5: 49-year-old man with VHLD.

A, Contrast-enhanced sagittal T1-weighted TSE image (700/12/3) shows a medium-sized, ovoid, heterogeneously enhancing tumor at T9. Note several small, homogeneously enhancing nodules cephalic to this tumor. Also note flow voids within the tumor and superficial enhancement of the spinal cord.

B, Contrast-enhanced axial T1-weighted SE image (660/15/1) shows the tumor at T9 occupies entire dural sac. The tumor was thought to be located deeply within the spinal cord, but turned out to be subpial in location at surgery.

The pathogenesis of syringeal formation in spinal hemangioblastoma remains unknown (15, 16). One hypothesis is that a syrinx is formed by a softening of the spinal cord resulting from damage to the cord or to the intramedullary vessels caused by the tumor. However, this mechanism is not likely in our cases, because a large syrinx was associated with even a tiny tumor that could hardly cause extensive damage to the spinal cord or intramedullary vessels. Samii et al (16) suggested that total or subtotal obstruction of CSF flow by an intramedullary tumor plays a major role in the development of a

syrinx. This mechanism was not the cause of the syringomyelia in our cases either, because most of the tumors were small and did not cause CSF obstruction. Transudation from the tumor vessels and secretion by tumor cells are generally believed to be the major causes of syringeal development in patients with intramedullary tumors (17, 18), and we speculate that this mechanism is most likely the cause of syringomyelia in spinal hemangioblastoma, because the tiny tumor would behave as a mural nodule of a cyst or syrinx, as frequently seen in cerebellar hemangioblastoma.

One may speculate that peritumoral edema leads to syringeal development; however, no such evidence has been reported to date. In our study, two patients who had edema were followed up by MR imaging, and in neither case did the edema change in extent or convert into a syrinx over a 2- or 3-year period, respectively (Figs 4 and 5). It is more likely that edema results from local venous congestion caused by the hypervascular tumor, which has arteriovenous shunts (4). Another hypothesis includes the production of an edema-promoting factor by the neoplasm. It is possible that hemangioblastomas secrete agents that induce increased capillary permeability (4).

The fourth characteristic MR finding observed in our study was the presence of vascular flow voids in or around medium-sized to large tumors (Figs 1, 6, and 8). This reflects distended feeding arteries or draining veins that were confirmed by angiography and/or surgery. We also found that tumor size was related to the tumor's shape, apparent location, signal intensity, homogeneity of enhancement, and the presence of vascular flow voids. When the tumor was small (10 mm or less), its shape was invariably nodular or ovoid, and its location was at the surface of the spinal cord or along a nerve root (Figs 3–7). When the tumor was larger than 10 mm, it was found either at the surface of or deep in the spinal cord, or it had an intra- and extramedullary location (exophytic growth), or was completely extramedullary in location (Fig 1). (It may be difficult to estimate the true location of a tumor that is larger than 10 mm, because the spinal cord may be compressed by the tumor and be barely recognizable on routine MR images.) Small tumors were primarily isointense on T1-weighted images and of high intensity on T2-weighted images (Fig 7), whereas larger tumors tended to be hypointense or mixed hypo- and isointense on T1-weighted images and of heterogeneous intensity on T2-weighted images (Figs 1 and 2). Most of the small tumors showed homogeneous enhancement, whereas medium-sized to large tumors tended to show heterogeneous enhancement (Figs 1, 2, 6, and 8).

In the present study, vascular flow voids were observed in or around the tumor in seven (58%) of the patients. We found that the vascular flow voids were absent when the tumor was less than 15 mm in size, whereas they were invariably present when the tumor size was 25 mm or greater. Therefore, a tumor is not likely to be a hemangioblastoma if it is 25 mm or larger and is not associated with vascular flow voids on MR images.

It has been reported that the diagnostic features of hemangioblastoma include the presence of enlarged arterial feeding vessels, a densely staining tumor nodule, and rapid shunt into a distended venous structure at angiography (1). In our study, MR imaging failed to detect dilated vessels in two medium-sized tumors (cases 9 and 10; 17 and 15 mm, respectively) and in one small tumor (case 7) that harbored abnormal vessels on angiograms. These results indicate that MR imaging underestimates the presence of dilated vessels. MR angiography is expected to have higher sensitivity in the detection of spinal vascular disease than conventional MR imaging. It has been reported that both phase-contrast MR angiography and 3D contrast-enhanced MR angiography have high accuracy in the characterization of spinal vascular disease and can depict the arterial pedicles, although the latter technique has shown better results (19, 20). Thus, MR angiography may be a good supplementary technique for characterizing spinal tumors, especially when vascular flow voids are indistinct on conventional MR studies. Although MR angiography may have sufficient spatial resolution for the detection of abnormal vascular structures, its time resolution is not sufficient to distinguish arterial feeders from draining veins. Moreover, acquisition time typically is longer than 20 seconds to obtain sufficient spatial resolution. Because MR angiography usually depicts arteries and venous structures simultaneously, it may be difficult to differentiate between feeding arteries and draining veins. In planning surgical treatment of a large hypervascular spinal tumor, it is essential to clarify the 3D relationship among tumor parenchyma, feeding arteries, and draining veins, because the main draining vein should not be interrupted before all feeding arteries have been completely devascularized by coagulation. If the main draining vein is coagulated before devascularization is complete, the change in hydrodynamics may increase the difficulty of the surgical procedure and damage the spinal cord (14). Piecemeal removal of the tumor should be avoided, because it may increase the possibility of tumor bleeding. Therefore, we believe that angiography is indicated for treatment planning when a large spinal tumor associated with vascular flow voids is found on MR images.

Angiography was performed in six of our patients (cases 3, 5, 6, 9, 10, and 11) to determine the location of feeding arteries and draining veins in order to plan a treatment strategy. In cases 3 and 6, the feeding arteries were embolized by using polyvinyl alcohol before surgery, and these tumors were removed safely by surgery. The ideal surgical procedure for spinal hemangioblastoma is to coagulate all feeding arteries before interrupting the main draining vein, and to remove the tumor en bloc. In some cases, distended draining veins reside

in front of the tumor and feeding arteries so that they hamper the surgical approach to feeding arteries. In such cases, we think that preoperative embolization of the feeding arteries is useful to reduce arterial flow and subsequently to shrink the draining veins and lower the risk of tumor bleeding. Chang et al (21) have shown that stereotactic radiosurgery provides a high likelihood of local control of hemangioblastoma and can be an alternative to multiple surgical procedures for patients with VHLD.

Although we do not consider that angiography is indicated for a small spinal tumor to confirm the diagnosis of hemangioblastoma, we performed angiography in one patient with a small tumor (case 7), because we initially had difficulty in reaching a diagnosis on MR images owing to a lack of experience early on. We did not perform angiography in case 8, because the tumor was small and located superficially at the posterior aspect of the spinal cord, and thus we expected the tumor to be excised easily and safely. Two patients (cases 1 and 5) declined to undergo angiography. We did not perform angiography in cases 2 and 4, because neither patient had subjective symptoms and the tumor was small; both were followed up with MR examinations.

Superficial enhancement of the spinal cord was concomitant with flow voids and was confirmed to be dilated perimedullary veins at surgery (Figs 1, 6, and 8). This finding may also be characteristic for spinal hemangioblastoma, although other spinal cord diseases with pial or subpial extension, such as high-grade astrocytoma, metastatic tumor, sarcoidosis, and tuberculosis, may have similar MR appearances.

In the present study, spinal hemangioblastomas were associated with VHLD in five (42%) of the 12 patients. We found that spinal hemangioblastomas in patients with VHLD were different from sporadic spinal hemangioblastomas only in their multiplicity and the size of the tumor. Multiple hemangioblastomas were found only in patients with VHLD. The percentage of small hemangioblastomas was significantly higher in patients with VHLD than in those without VHLD. This was because the asymptomatic hemangioblastomas were found incidentally on MR examinations performed for other symptomatic tumors, or they were found on the screening examination for CNS tumors in patients with VHLD. There was no difference in the other MR features between the two groups.

No differences were found in symptoms between the patients with and without VHLD. The main symptoms included pain, proprioceptive sensation disturbance of position and vibration, motor weakness, and bowel and urinary dysfunction. These manifestations are consistent with previous findings (1).

In the patients with VHLD, most small tumors (10 mm or less) were considered asymptomatic. Solitary spinal hemangioblastoma was found in one patient with VHLD and in seven patients without VHLD. Two of these patients had asymptomatic tumors, 6 and 15 mm in size, respectively. It is noteworthy that spinal hemangioblastoma was found incidentally even in a patient without VHLD. This relatively high rate of occurrence of asymptomatic hemangioblastoma is attributable to the high detectability of spinal tumors by MR imaging. We thus suggest that in patients with VHLD the entire neuraxis should be screened by MR imaging for potential association of hemangioblastoma, even when neurologic symptoms are absent. Contrast-enhanced T1-weighted imaging is most appropriate for this purpose, because it is the most sensitive in detecting small hemangioblastomas.

In cases of small tumors, clinical symptoms were believed to be caused by the associated syrinx and not by the tumor itself. As for medium-sized to large tumors, the clinical symptoms were attributable to the syrinx or to the tumor itself. Peritumoral edema without syrinx did not contribute to the patients' symptoms. We speculate that the small tumors without associated syrinx did not damage the spinal cord, because their location was completely subpial. When a tumor becomes larger, it will cause symptoms by virtue of its mass effect on the spinal cord. The fact that a small subpial hemangioblastoma without an associated syrinx is asymptomatic may be important in differentiating other diseases, which may produce small, enhancing foci (with or without spinal cord edema), such as metastatic tumors, sarcoidosis, tuberculosis, neurosyphilis, fungal infection, and multiple sclerosis, because these diseases may be symptomatic even when their enhancing lesions are small.

In general, the differential diagnosis of spinal tumors is based primarily on the location of the tumor on imaging studies. On MR images, an intramedullary tumor is most likely a hemangioblastoma when it is small, well demarcated, intensely enhanced, located at the surface of the spinal cord, and associated with a relatively large syrinx. Peritumoral edema is not always present. When the patient is asymptomatic, syrinx may be absent. As for an intramedullary tumor larger than 10 mm, it is most likely a hemangioblastoma when an associated syrinx and vascular flow voids are present in or around the tumor. Spinal hemangioblastoma can also be found either in an intradural extramedullary or an extradural location (1, 2, 8, 14). It can arise from filum terminale, intradural nerve roots, extradural nerves, or it can exist independent of these structures. The distinguishing MR feature of a hemangioblastoma in these locations is the presence of vascular flow voids. However, when vascular flow voids are present on MR images, spinal hemangioblastomas should be differentiated from arteriovenous malformations (AVMs) and other hypervascular tumors, including paraganglioma and metastatic tumors (especially from renal cell carcinomas), that frequently occur in patients with VHLD (5, 8, 14, 22). A well-defined enhancing mass should serve to distinguish spinal tumors from AVMs (14).

A thorough search for a primary tumor, such as a renal carcinoma, is necessary, especially in patients with VHLD. Spinal paragangliomas are usually found in the intradural extramedullary compartment (22) and are difficult to differentiate from extramedullary hemangioblastoma.

Conclusion

MR features of spinal hemangioblastoma depend on the size of the tumor. Small (10 mm or less) hemangioblastomas are mostly isointense on T1-weighted images and hyperintense on T2-weighted images and show homogeneous enhancement, whereas larger ones tend to be hypointense or mixed hypo- and isointense on T1-weighted images and heterogeneous on T2-weighted images, and tend to show heterogeneous enhancement. Small hemangioblastomas are located at the surface of the spinal cord, most frequently at the posterior aspect, and show well-demarcated, intense enhancement. A hemangioblastoma larger than 24 mm is accompanied by vascular flow voids on MR images. Symptomatic small hemangioblastomas have a relatively large associated syrinx. Asymptomatic hemangioblastomas do not have an associated syrinx, although they may have peritumoral edema. Spinal hemangioblastomas in patients with VHLD tend to be multiple. Although the percentage of small hemangioblastomas is significantly higher in patients with VHLD than in those without VHLD, there is no difference in the other MR findings between the two groups. Because asymptomatic hemangioblastomas are frequently found in patients with VHLD, the entire neuraxis should be screened by contrast-enhanced MR imaging. Knowledge of these MR features helps to differentiate spinal hemangioblastomas from other spinal tumors and other diseases that produce enhancing nodules. Angiography is indicated for treatment planning when a large spinal tumor associated with vascular flow voids is found on MR images.

References

1. Browne TR, Adams RD, Roberson GH. **Hemangioblastoma of the spinal cord: review and report of five cases.** *Arch Neurol* 1976;33:435–441
2. Wisoff HS, Suzuki Y, Llena JF, Fine DIM. **Extramedullary hemangioblastoma of the spinal cord.** *J Neurosurg* 1978;48:461–464
3. Corr P, Dicker T, Wright M. **Exophytic intramedullary hemangioblastoma presenting as an extramedullary mass on myelography.** *AJNR Am J Neuroradiol* 1995;16:883–884
4. Solomon RA, Stein BM. **Unusual spinal cord enlargement related to intramedullary hemangioblastoma.** *J Neurosurg* 1988; 68:550–553
5. Sato Y, Waziri M, Smith W, et al. **Hippel-Lindau disease: MR imaging.** *Radiology* 1988;166:241–246
6. Kaffenberger DA, Shah CP, Murtagh FR, et al. **MR imaging of spinal cord hemangioblastoma associated with syringomyelia.** *J Comput Assist Tomogr* 1988;12;495–498
7. Murota T, Symon L. **Surgical management of hemangioblastoma of the spinal cord: a report of 18 cases.** *Neurosurgery* 1989; 25:699–708
8. Arbelaez A, Castillo M, Armao D. **Hemangioblastoma of the filum terminale: MR imaging.** *AJR Am J Roentgenol* 1999;173: 857–858
9. Silbergeld J, Cohen WA, Maravilla KR, et al. **Supratentorial and spinal cord hemangioblastomas: gadolinium enhanced MR appearance with pathologic correlation.** *J Comput Assist Tomogr* 1989;13:1048–1051
10. Friedman DP, Flanders AE, Tartaglino LM. **Vascular neoplasms and malformations, ischemia, and hemorrhage affecting the spinal cord: MR imaging findings.** *AJR Am J Roentgenol* 1994; 162:685–692
11. Yu JS, Short MP, Schumacher J, et al. **Intramedullary hemorrhage in spinal cord hemangioblastoma.** *J Neurosurg* 1994;81: 937–940
12. Neumann HPH, Eggert HR, Weigel K, et al. **Hemangioblastomas of the central nervous system: a 10-year study with special reference to von Hippel-Lindau syndrome.** *J Neurosurg* 1989; 70:24–30
13. Baker KB, Moran CJ, Wippold FJ II, et al. **MR imaging of spinal hemangioblastoma.** *AJR Am J Roentgenol* 2000;174:377–382
14. Xu QW, Bao WM, Mao RL, Yang GY. **Magnetic resonance imaging and microsurgical treatment of intramedullary hemangioblastoma of the spinal cord.** *Neurosurgery* 1994;35:671–676
15. Enomoto H, Shibata T, Ito A, et al. **Multiple hemangioblastomas accompanied by syringomyelia in the cerebellum and the spinal cord.** *Surg Neurol* 1984;22:197–203
16. Samii M, Klekamp J. **Surgical results of 100 intramedullary tumors in relation to accompanying syringomyelia.** *Neurosurgery* 1994;35:865–873
17. Gardner WJ. **Hydrodynamic mechanism of syringomyelia: its relationship to myelocele.** *J Neurol Neurosurg Psychiatry* 1965; 28:247–259
18. Kiwitt JCW, Lanksch WR, Fritsch H, et al. **Magnetic resonance tomography of solid spinal cord tumors with extensive secondary syringomyelia.** *Adv Neurosurg* 1988;16:211–215
19. Mascalchi M, Quilici N, Ferrito G, et al. **Identification of the feeding arteries of spinal vascular lesions via phase-contrast MR angiography with three-dimensional acquisition and phase display.** *AJNR Am J Neuroradiol* 1997;18:351–358
20. Binkert CA, Kollias SS, Valavanis A. **Spinal cord vascular disease: characterization with fast three-dimensional contrast-enhanced MR angiography.** *AJNR Am J Neuroradiol* 1999;20: 1785–1793
21. Chang SD, Meisel JA, Hancock SL, et al. **Treatment of hemangioblastomas in von Hippel-Lindau disease with linear accelerator-based radiosurgery.** *Neurosurgery* 1998;43:28–35
22. Sundgren P, Annertz M, Englund E, et al. **Paragangliomas of the spinal canal.** *Neuroradiology* 1999;41:788–794